Published in final edited form as:
Nano Lett. 2008 October ; 8(10): 3310–3314. doi:10.1021/nl801693k.

Label-free Electronic Detection of the Antigen-Specific T-Cell Immune Response

Eric Stern[†], **Erin R. Steenblock**[†], **Mark A. Reed**[*,‡,§], and **Tarek M. Fahmy**[*,†,‖]

[†]Department of Biomedical Engineering, Yale University, 55 Prospect Street, New Haven, Connecticut 06511

[‡]Department of Electrical Engineering, Yale University, 55 Prospect Street, New Haven, Connecticut 06511

[§]Department of Applied Physics, Yale University, 55 Prospect Street, New Haven, Connecticut 06511

[‖]Department of Chemical Engineering, Yale University, 55 Prospect Street, New Haven, Connecticut 06511

Abstract

Detection of antigen-specific T-cells is critical for diagnostic assessment and design of therapeutic strategies for many disease states. Effective monitoring of these cells requires technologies that assess their numbers as well as functional response. Current detection of antigen-specific T-cells involves flow cytometry and functional assays and requires fluorescently labeled, soluble forms of peptide-loaded major histocompatability complexes (MHC). We demonstrate that nanoscale solid-state complementary metal-oxide-semiconductor (CMOS) technology can be employed to allow direct, label-free electronic detection of antigen-specific T-cell responses within seconds after stimulation. Our approach relies on detection of extracellular acidification arising from a small number of T-cells (as few as ~200), whose activation is induced by triggering the T-cell antigen receptor. We show that T-cell triggering by a nonspecific anti-CD3 stimulus can be detected within 10 s after exposure to the stimulus. In contrast, antigen-specific T-cell responses are slower with response times greater than 40 s after exposure to peptide/MHC agonists. The speed and sensitivity of this technique has the potential to elucidate new understandings of the kinetics of activation-induced T-cell responses. This combined with its ease of integration into conventional electronics potentially enable rapid clinical testing and high-throughput epitope and drug screening.

The cellular response of antigen-specific $CD8^+$ or $CD4^+$ T-cells is mediated by the interaction of the T-cell antigen receptor with peptide-loaded major histocompatability complexes (peptide/MHC Class I or II, respectively) displayed on the surface of antigen presenting cells.[1] Recognition of these complexes by T-cells triggers a signaling cascade leading to activation and proliferation of effector T-cell populations. Detection of such T-cell subsets, which currently requires the use of labeled probes in conjunction with immunofluorescence and functional assays,[2–6] allows monitoring of antigen-induced immunity and is critical to understanding the natural course and designing efficient strategies for immune modulation and intervention.[7,8] Peptide-MHC tetramers[7,9] and dimers[8,10] that bind to the T-cell receptor with high affinity have emerged as powerful tools for enumeration of the frequency and phenotype of specific T-cells in a variety of applications, including autoimmune disease and cancer.[8,9]

*To whom correspondence should be addressed.

Rapid and inexpensive detection of antigen-specific T-cells upon exposure to antigens may offer the potential for point-of-care clinical testing.[11–14] However, current state-of-the-art technologies are laborious and require large numbers of cells and, most critically, do not validate a functional cellular response. Such validation is critical for assessing cells' therapeutic value in different disease states because antigen-specific T-cells may be present in an anergic state, and, hence, fail to undergo stimulus-induced activation.[14] Although the recent innovation of patterned MHC arrays has enabled high-throughput testing of rare T-cell populations,[5] the reliance on fluorescent biomarkers to determine cellular functionality may limit applications. Here, we use a label-free sensing platform with a direct electronic readout to discriminate between specific T-cell populations within seconds. The speed, sensitivity, and ease of detection with this approach render it ideal for eventual point-of-care settings.[15]

Nanowire-field effect transistor (NW-FET) devices have been recently demonstrated as ultrasensitive sensors for unlabeled reagents.[15–17] The current in a NW-FET (the "channel current") is dependent upon the amount of charge surrounding the device. The addition or removal of surface charges to these solid state devices modulates the channel current, thereby producing a direct electrical readout of bound charged species. The large surface area-to-volume ratio of NW-FETs maximizes the effect of surface charge on channel current, which in turn maximizes device sensitivity.[15–17] These devices are thus ideally suited for biomolecular sensing. Since the NW-FET surface is composed of silanol groups (hydroxyl groups bound to silicon), when configured as solution-phase sensors these devices are ideal for monitoring pH changes,[15] enabling real-time monitoring of cellular metabolic activity.[18–20] Live cellular measurements can be performed in buffers with physiologic salt concentrations (~150 mM) because monitoring protonation and deprotonation on the NW-FET surface eliminates concerns over Debye screening, as these events occur well within the ~0.7 nm Debye screening length.[21]

We recently reported the complete fabrication of NW-FET sensors using conventional lithographic techniques (complementary metal-oxide-semiconductor, CMOS technology).[15] The use of CMOS technology to create such devices is critical because it enables sensors to not only be manufactured with high repeatability but also to be seamlessly integrated into on-chip electronics for signal processing. Thus, this device platform requires only minimal, inexpensive additional hardware. Here we demonstrate the applicability of this approach in detection of the antigen-specific immune response. We show that the enhanced temporal response of these devices enables, for the first time, direct electronic label-free detection within ~1 s of stimulus-induced antigen-specific T-cell responses, a resolution previously only accessible with labeled assays. Additionally, the increased sensitivity of NW-FET sensors enables a response to be detected from ~210 cells, fewer than ever previously reported with label-free approaches.

An optical micrograph of a completed device and reservoir is shown (Figure 1A). The reservoir is filled with a cell suspension to which the protein stimulus is introduced by direct injection with a pipet. Thus, no solution exchange occurs (no cells are added or removed; see Supporting Information, Figure 1). Mixing of the solution in the reservoir is performed manually with a micropipette for uniform delivery of the stimulus to all cells. The native sensor characteristics (the dependence of source-drain current (I_{SD}) on source-drain voltage (V_{SD}) for varying gate-drain voltage (V_{GD})) are shown in Figure 1B for a representative p-type device.[15] As the negative charge surrounding the device increases (becomes more negative), achieved by making V_{GD} more negative, the current flowing through the device (I_{SD}) increases for all V_{SD}. The inset in Figure 1B shows the $I_{SD}(V_{GD})$ characteristic for $V_{SD} = -10V$ for the same device.

Previous studies have demonstrated extracellular acidification within three minutes as a result of specific (peptide/MHC) or nonspecific (mouse-anti-CD3ϵ, anti-CD3) T-cell activation.[19] As illustrated schematically in Figure 1C, cellular release of protons in response to T-cell stimulation results in protonation of the silanol groups of the NW-FET. The resulting decrease in negative charge on the surface of the p-type NW-FET results in a decrease in the magnitude of the source-drain current, $|I_{SD}|$. All subsequent data plots in this work define *time* = 0 as the moment of protein or acid injection.

The system response time was investigated by directly lowering the pH of the solution in the reservoir. An acidic solution consisting of dilute hydrochloric acid dissolved in a 150 mM sodium chloride solution was added to and mixed with a weakly buffered solution present in the reservoir, resulting in a pH decrease of 0.5 units. The weakly buffered solution was obtained by making a 1:10 dilution of 1X phosphate buffered saline (PBS) in 150 mM sodium chloride. The final current level is reached ~1.5 s after acid addition (Figure 2A). The stability of the device current after this 1.5 s transient indicates that solution mixing occurred within this time frame. Thus, longer response times observed in experiments involving cell stimulation are due to the time required for cellular metabolic activity to result in extracellular acidification.

Initial experiments focused on the utility of the device for detecting proton secretion due to activation-induced polyclonal T-cell signaling. Splenocytes isolated from a C57BL/6 (B6) mouse were suspended in a low-buffered solution and stimulated with anti-CD3 antibody. Extracellular acidification was observed to begin ~8 s after injection (Figure 2B). Our previous characterization of a 1.5 s device response time indicated that the ~8 s delay observed in Figure 2B was primarily due to intrinsic cellular processes. To ensure that extracellular pH changes were due to stimulation-induced cellular metabolic activity, we treated splenocytes derived from the same mouse with genistein, a tyrosine kinase inhibitor that inhibits the induced intracellular signaling cascade without affecting cellular viability.[19] In separate experiments, we noted that genistein, at the concentration used in this study, did not affect cell viability as assessed by trypan-blue staining. In the presence of genistein, addition of anti-CD3 antibody resulted in no change in solution pH (Figure 2B). This confirms that the positive response observed in untreated cells is due to anti-CD3 antibody-initiated proton secretion from splenocytes, consistent with previous findings.[15,19,20]

We next investigated the ability of this system to discriminate between well-established peptide-specific MHC restricted responses of T-cell clones. We stimulated murine splenocytes isolated from 2C and OT-1 transgenic mice with dimeric MHC ligands presenting their cognate and noncognate peptides. 2C and OT-1 $CD8^+$ T-cells (cytotoxic Tlymphocytes, CTLs) react against a broad range of defined peptides presented by syngeneic MHC Class I, H-$2K^b$. OT-1 mice, expressing a transgene for the T-cell antigen receptor, are reactive with the complex of H-$2K^b$ and the ovalbumin octapeptide SIINFEKL ($^{SIIN}K^b$, ref [22]). As a negative control for this system, we used a noncognate peptide derived from a peptide library, SIYRYYGL ($^{SIY}K^b$). Cytotoxic T-lymphocytes from 2C transgenic mice should be reactive to $^{SIY}K^b$ but exhibit a null response to $^{SIIN}K^b$ (ref [23]). Using a NW-FET sensor, we observed a drop in solution pH beginning ~40 s after addition of $^{SIIN}K^b$ dimer to OT-1 splenocytes; no response was observed after addition of $^{SIY}K^b$ (Figure 3A). Conversely, 2C CTLs reacted to the presence of the $^{SIY}K^b$ with proton secretion beginning ~40 s after peptide/MHC addition. The device showed no discernible changes in conductance when $^{SIIN}K^b$ was added to 2C splenocytes (Figure 3B). Different devices were used in each panel of Figure 2 and Figure 3 but each plot contains data from a single device. Variations in conductance and conductance changes observed between panels are due to device-to-device variation.

The observation that onset of extracellular acidification of T-cells upon stimulation with peptide/MHC after a lag of ~40 s was longer than that measured for anti-CD3 antibody

stimulation, ~8 s. There are two candidate mechanisms potentially responsible for the observed delay: (1) the kinetics of T-cell activation are strongly affected by the dwell time of the T-cell receptor-activating stimulus.[24–26] Antibodies that trigger the CD3 complex bind with higher affinities (K_d~ 1–10 nM) than peptide/MHC dimers (K_d ~ 50–150 nM), which may lead to faster intracellular signaling, resulting in earlier acid release.[27,28] (2) A smaller population of responsive cells (typically ~20–30% of all transgenic splenocytes are reactive to the specific antigen) may require a longer time for accumulation of the signaling molecules needed to achieve sufficient extracellular acidification.

We distinguished between these possible mechanisms by stimulating dilutions of OT-1 cells mixed with background splenocytes derived from B6 mice. Upon stimulation with cognate antigen ($^{SIIN}K^{b}$), we observed a decrease in device signal intensity with decreasing numbers of OT-1 cells, Figure 3C. The observed responses were produced by OT-1 splenocyte populations of approximately 28 000, 7000, and 700 cells for the 1:3, 1:10, and 1:100 dilutions, respectively. The onset of stimulus-induced extracellular acidification began ~45–49 s for all dilutions, indicating that the strength of the stimulus, rather than changes in the cell density, was responsible for the delay. These data are consistent with previous studies that monitored the dynamics of intracellular calcium flux (which had similar response times[5]) after stimulation with different agonists and showed that the apparent lag time after antigen-specific T-cell triggering correlated with signal strength.[29]

The approach described in this report is well suited for label-free detection of stimulus-induced extracellular acidification within seconds after stimulation of a small number of cells, <210 (30% of 700). Though this work focuses on one specific cell type with variable specificities, it can be extrapolated to other systems because extracellular release of protons is triggered by a general signal transduction pathway as a result of the production of acidic metabolites or the activation of proton membrane transporters.[30] Nano-wire-FET sensor sensitivity, rapid response time, small required sample volume, suitability for high-throughput analysis, and potential for integration into full electronic on-chip systems position this technology for seamless application into basic and clinical settings requiring detection of T-cell antigen-specific responses.

Supplementary Material

Refer to Web version on PubMed Central for supplementary material.

Acknowledgment

The authors would like to thank Rob Ilic, Daron Westly, Meredith Metzler, and Vincent Genova of the Cornell Nanofabrication Facility for device processing assistance; Guosheng Cheng, James Hyland, Michael Young, Christopher Tillinghast, James Klemic, and David Routen-berg for helpful device processing discussions; Johnathan Schneck (Johns Hopkins School of Medicine) for providing dimeric MHC complexes; Howard Eisen (MIT) for his generous gift of mouse 2C splenocytes and helpful discussions; and David Stern for sensing discussions and assistance in manuscript preparation. This work was partially supported by DARPA through ONR and AFOSR (M.A.R.), NASA (M.A.R.), ARO (M.A.R.), NIH R01 (EB008260-01) (M.A.R. and T.M.F.), by Department of Homeland Security graduate fellowships (E.S. and E.R.S.), and by a NSF graduate fellowship (ES). This work was performed in part at the Cornell Nanoscale Science and Technology Facility, a member of the National Nanotechnology Infrastructure Network that is supported by the NSF.

References

1. Margulies, DM.; McCluskey, J. Fundamental Immunology. Paul, WE., editor. Philadelphia: Lippincott-Raven; 1999. p. 267-289.
2. Slansky JE. PLoS Biol 2003;1:e78. [PubMed: 14691549]
3. Sallusto F, Geginat J, Lanzavecchia A. Annu. ReV. Immunol 2004;22:745–763. [PubMed: 15032595]

4. Lanzavecchia A. EmBo J 1998;7:2945–2951. [PubMed: 3053159]
5. Soen Y, Chen DS, Kraft DL, Davis MM, Brown PO. PLoS Biol 2003;1:e65. [PubMed: 14691537]
6. Chen DS, Davis MM. Curr. Opin. Chem. Biol 2006;10:28–34. [PubMed: 16413817]
7. Altman JD, Moss PAH, Goulder PJR, Barouch DH, McHeyzer-Williams MG, et al. Science 1996;274:94–96. [PubMed: 8810254]
8. Howard MC, Spack EG, Choudhury K, Greten TF, Schneck JP. Immunol. Today 1999;20:161–165. [PubMed: 10203711]
9. Klenerman P, Cerundolo V, Dunbar PR. Nature ReV. Immunol 2002;2:263–272. [PubMed: 12001997]
10. Crawford F, Kozono H, White J, Marrack P, Kappler J. Immunity 1998;8:675–682. [PubMed: 9655481]
11. Chen DS, Davis MM. Springer Semin. Immunopathol 2005;27:119–127. [PubMed: 15834723]
12. Lee PP, Yee C, Savage PA, Fong L, Brockstedt D, Weber JS, Johnson D, Swetter S, Thompson J, Greenberg PD, Roederer M, Davis MM. Nat. Med 1999;5:677–685. [PubMed: 10371507]
13. Zippelius A, Batard P, Rubio-Godoy V, Bioley G, Lienard D, Lejeune F, Rimoldi D, Guillaume P, Meidenbauer N, Mackensen A, Rufer N, Lubenow N, Speiser D, Cerrottini J-C, Romero P, Jittet MJ. Cancer Res 2004;64:2865–2873. [PubMed: 15087405]
14. Chen DS, Davis MM. Curr. Opin. Chem. Biol 2006;10:28–34. [PubMed: 16413817]
15. Stern E, Klemic JF, Routenberg DA, Wyrembak PN, Turner-Evans DB, Hamilton AD, LaVan DA, Fahmy TM, Reed MA. Nature 2007;445:519–522. [PubMed: 17268465]
16. Bunimovich YL, Shin YS, Yeo WS, Amori M, Kowng G, Heath JR. J. Am. Chem. Soc 2007;128:16323–16331. [PubMed: 17165787]
17. Li C, Curreli M, Lin H, Lei B, Ishikawa FN, Datar R, Cote RJ, Thompson ME, Zhou C. J. Am. Chem. Soc 2005;127:12484–12485. [PubMed: 16144384]
18. McConnell HM, Owicki JC, Parce JW, Miller DL, Baxter GT, Wada HG, Pitchford S. Science 1992;257:1906–1912. [PubMed: 1329199]
19. Nag B, Wada HG, Fok KS, Green DJ, Sharma SD, Clark BR, Parce JW, McConnell HM. J. Immunol 1992;148:2040–2044. [PubMed: 1372021]
20. Owicki JC, Parce JW, Kercso KM, Sigal GB, Muir VC, Fraser CM, McConnell HM. Proc. Natl. Acad. Sci. U.S.A 1990;87:4007–4011. [PubMed: 2160082]
21. Stern E, Wagner R, Sigworth FJ, Breaker R, Fahmy TM, Reed MA. Nano Lett 2007;7:3405–3409. [PubMed: 17914853]
22. Hogquist KA, Jameson SC, Heath WR, Howard JL, Bevan MJ, Carbone FR. Cell 1994;76:17–27. [PubMed: 8287475]
23. Udaka K, Wiesmuller KH, Kienle S, Jung G, Walden P. 1996;157:670–678.
24. Kalergis AM, Boucheron N, Doucey MA, Palmieri E, Goyarts EC, Vegh Z, Luescher IF, Nathenson SG. Nat. Immunol 2001;2:229–234. [PubMed: 11224522]
25. Lanzavecchia A, Iezzi G, Viola A. Cell 1999;96:1–4. [PubMed: 9989490]
26. Matsui K, Boniface JJ, Steffner P, Reay PA, Davis MM. Proc. Natl. Acad. Sci. U.S.A 1994;91:12862–12866. [PubMed: 7809136]
27. Hennecke J, Wiley DC. Cell 2001;104:1–4. [PubMed: 11163234]
28. Fahmy TM, Bieler JG, Edidin M, Schneck JP. Immunity 2001;14:135–143. [PubMed: 11239446]
29. Wulfing C, Rabinowitz JD, Beeson C, Sjaastad MD, McConnell HM, Davis MM. J. Exp. Med 1997;185:1815–1825. [PubMed: 9151707]
30. Wada HG, Indelicato SR, Meyer L, Kitamura T, Miyajima A, Kirk G, Muir VC, Parce JW. J. Cell Physiol 1993;154:129–138. [PubMed: 7678263]

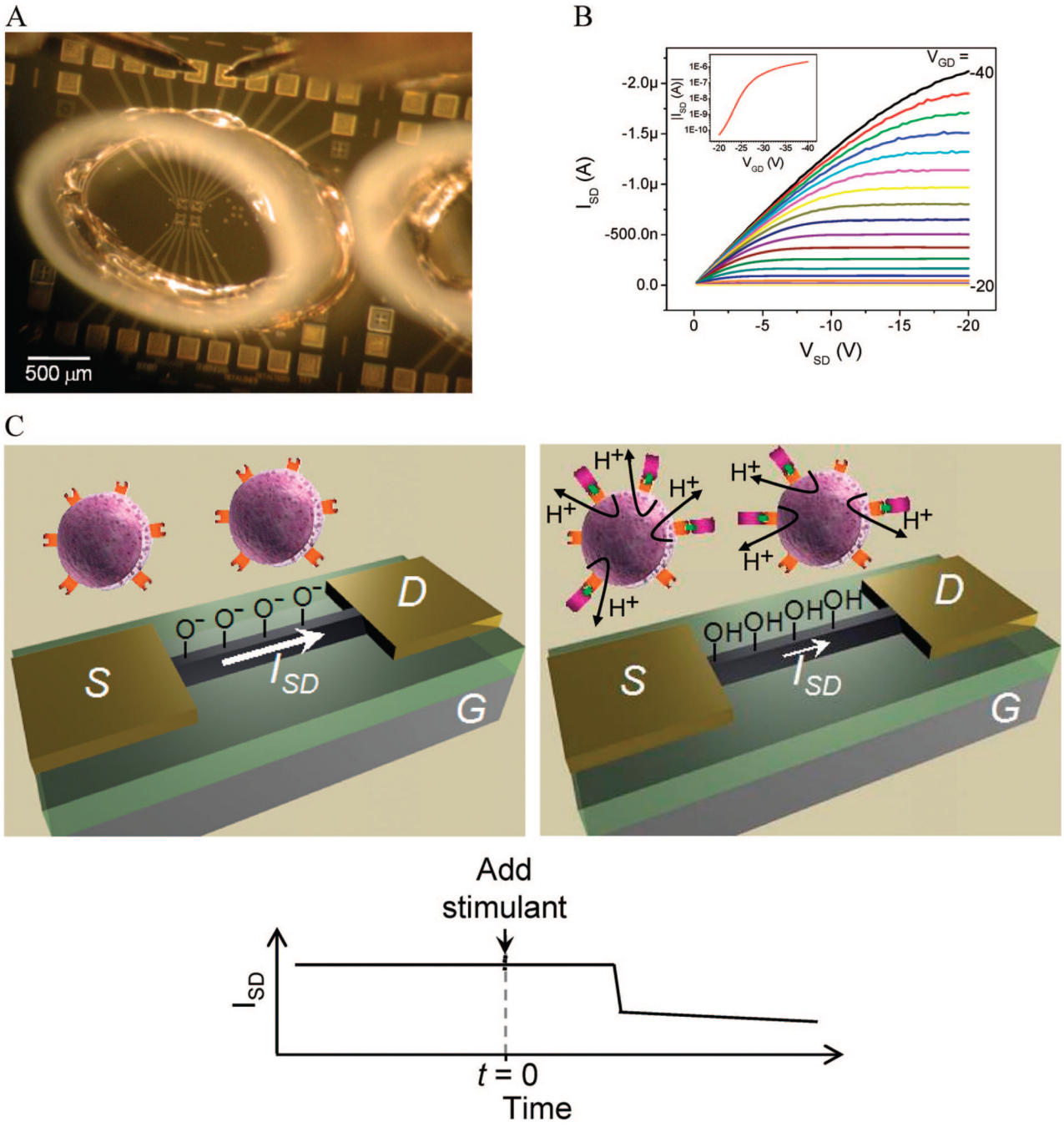

Figure 1. Measurement system

(A) Optical micrograph of a NW-FET sensor array with fluid reservoir attached and source and drain contacted. (B) $I_{SD}(V_{SD}, V_{GD})$ characteristics for a representative device in ambient conditions; inset shows the subthreshold characteristics for the same device. (C) Sensing schematic: pre-T-cell stimulation (left) and poststimulation and activation (right). Prior to T-cell activation, a majority of the nanowire's silanol groups (active region colored black) are deprotonated. After activation, extracellular acidification results in increased protonation of the surface silanol groups, which decreases $|I_{SD}|$ ($|I_{SD}|$ vs time plot). The time required for T-cell activation after stimulant addition can be quantified.

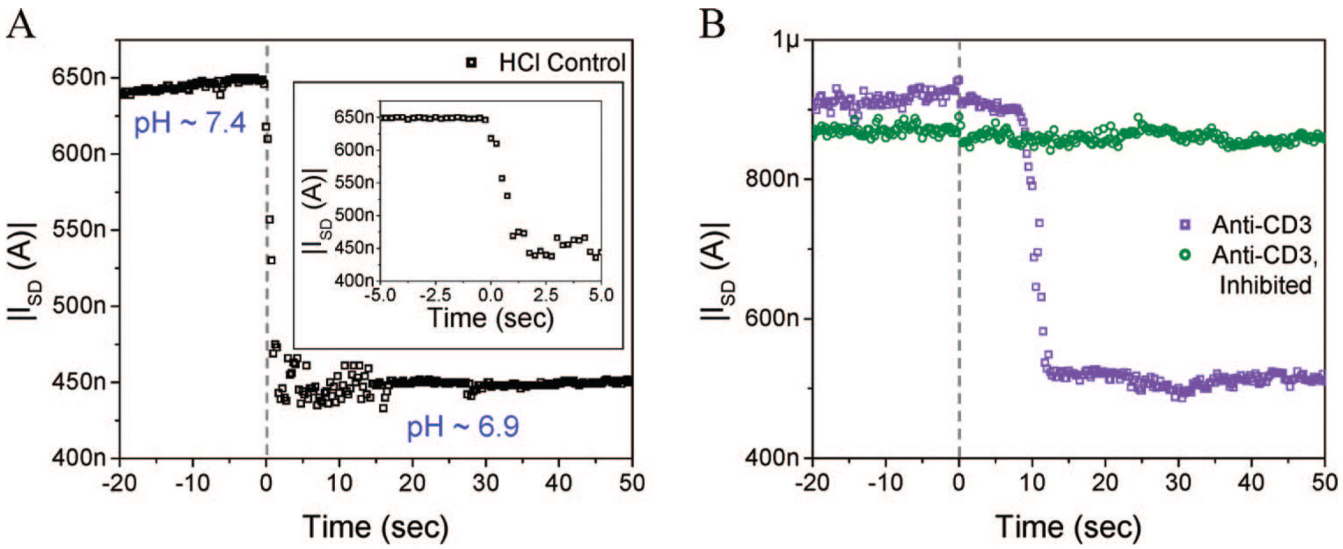

Figure 2. Characterization of T-cell activation

(A) Device response to the addition of 1 mL of dilute hydrochloric acid to a cell-free buffer, demonstrating system response of ~1.5 s; the inset highlights this delay time. Solution pH values are given in the figure. (B) Measurement of extracellular acidification upon stimulation of B6 splenocytes with anti-CD3. The T-cell response time is ~8 s. Pretreatment of splenocytes with genistein (50 mg/mL), which inhibits cell signaling, eliminates anti-CD3 induced cellular metabolic activity.

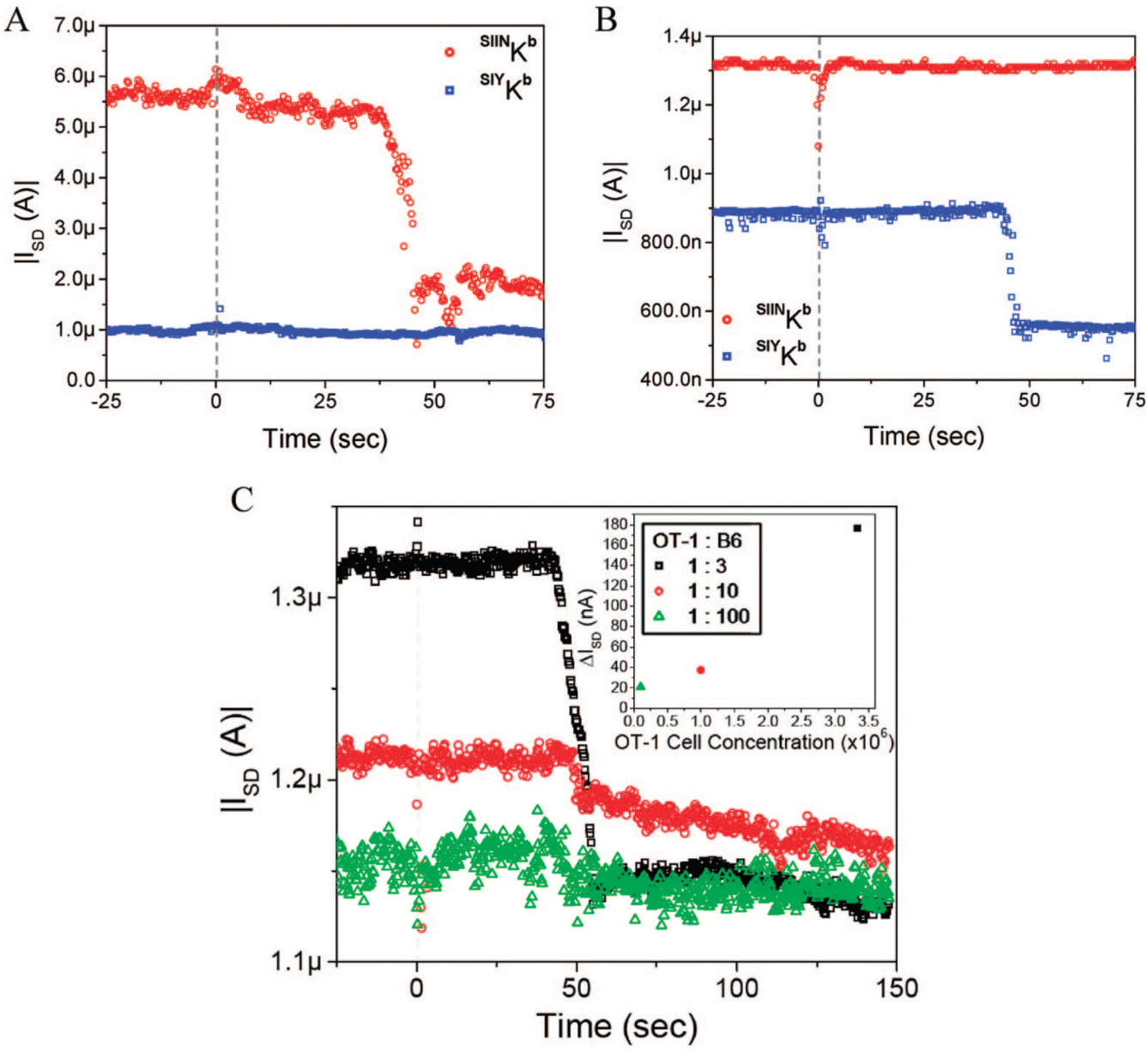

Figure 3. Antigen-specific CTL response

(A) OT-1 and (B) 2C splenocytes stimulated with $^{SIIN}K^b$ and $^{SIY}K^b$ dimeric constructs. For both positively stimulated splenocyte populations (OT-1 with $^{SIIN}K^b$ and 2C with $^{SIY}K^b$), extracellular acidification began at ~40 s. Different devices were used for each measurement. (C) OT-1 splenocytes were diluted at various ratios with wild-type B6 splenocytes; CTL response to stimulation with $^{SIIN}K^b$ was measured. The $|I_{SD}|$ values before and after the onset of extracellular acidification are significantly different at the 99.9% confidence level for all dilutions (*t* test). The same device was used for all measurements. No significant response was observed for a 1:1000 dilution. The inset shows a plot of the observed change in $|I_{SD}|$ versus the OT-1 cell concentration for these measurements.